

Tissue distribution, metabolism and excretion of paclitaxel in mice

Alex Sparreboom, Olaf van Tellingen, Willem J Nooljen and Jos H Beijnen¹

Department of Clinical Chemistry, Antoni van Leeuwenhoek Huis, The Netherlands Cancer Institute, Plesmanlaan 121, 1066 CX Amsterdam, The Netherlands. Tel: (+31) 20 5122792; Fax: (+31) 20 6172625.

¹ Department of Pharmacy, Slotervaart Hospital, Louwesweg 6, 1066 EC, Amsterdam, The Netherlands.

So far, all animal pharmacokinetic studies of paclitaxel, which used analytical procedures based on HPLC, have not been sensitive enough to quantify drug levels below 500 ng/ml. Consequently, the interpretation of the results is restricted because drug levels of paclitaxel as low as at least 50 nM (43 ng/ml) are relevant for the pharmacology of this drug. We recently described an accurate and very sensitive method based on HPLC for the determination of paclitaxel and the metabolites 3'-*p*-hydroxypaclitaxel (I), 6 α -hydroxypaclitaxel (II) and 6 α ,3'-*p*-dihydroxypaclitaxel (III) in a wide variety of biological matrices. We have now implemented this methodology in a comprehensive pharmacokinetic study in female FVB mice. Previous pharmacokinetic studies in humans demonstrated a large steady-state volume of distribution, indicating that the drug is widely distributed into tissues. Comprehensive tissue distribution studies may, therefore, be helpful in providing more insight into possible relationships between plasma levels, drug levels in tissues and toxicity. Paclitaxel, formulated in Cremophor EL and ethanol (1:1, v/v), was given as a single i.v. bolus dose of 2, 10 and 20 mg/kg to female FVB mice. Except for the brain, the distribution of paclitaxel to all other tissues in the female mice was substantial and maximum drug levels were achieved within 0.5 or 1 h. A marked non-linear increase in the area under the concentration-time curve (AUC) in plasma was observed, which was not paralleled by a proportional increase in the tissue AUC levels. It is postulated that this effect may be related to the substantial amounts of Cremophor EL administered concurrently. The recovery of paclitaxel in the feces (0–96 h) was reduced from 58% at the 2 mg/kg dose level to 44% at the 20 mg/kg dose level. Small amounts of metabolites I and II were detected in the gut, liver and gall bladder, but not in the systemic circulation or any other tissue. Metabolite III was not detected. Metabolites I and II are likely excreted directly into the bile, and since their recovery in the feces accounts for about 25% of the administered dose, their formation thus represents an important pathway of detoxification.

Key words: Disposition, excretion, metabolism, mice, paclitaxel (Taxol®).

Introduction

Since the initial reports on the promising activity of paclitaxel in the treatment of advanced ovarian cancer,¹ the drug has evoked widespread enthusiasm as indicated by the great number of studies which have been reported since. These studies have demonstrated the efficacy of the drug in the treatment of a number of solid tumors, including breast cancer,² non-small cell lung cancer³ and leukemia,⁴ and indicate that paclitaxel possesses antitumor activity against a relatively broad spectrum of malignancies. These clinical results correspond with results which have been obtained in a diverse array of experimental tumor models.⁵ Currently, optimization of the usage of this drug is pursued, for instance by testing the efficacy of paclitaxel in combination chemotherapy, by further dose escalation in combination with hematopoietic growth factors and/or by utilization of long-term infusion schedules.

Due to the substantial number of clinical trials, which have included drug monitoring in plasma, the pharmacokinetic behavior of paclitaxel in humans has now been reasonably well defined (for an overview see Spencer *et al.*⁶). The volume of distribution for paclitaxel is high, indicating extensive tissue distribution. In particular, when paclitaxel is infused over a short period (3 h), non-linear pharmacokinetic behavior is noted, whereas when the same dose was infused over 24 h, this effect was less.^{7–11} However, at similar dose levels the latter schedule resulted in more severe toxic side effects. Based on these results we postulated that the toxicity is related with the time that the drug exceeds a threshold level of 100 nM (86 ng/ml).⁷ Although other groups, by using more refined statistical methods, have shown that 50 nM is a more appropriate concentration,^{10,11} the idea of a threshold level has now become generally accepted. The consequences of non-linear pharmacokinetic behavior and toxicity, however, remain unclear.

Correspondence to Alex Sparreboom

Comprehensive pharmacokinetic studies, focused in particular on tissue distribution, are important for improving our knowledge on the relations between pharmacokinetics and pharmacodynamics, and thus for the design of more efficacious treatment schedules. Because such studies are difficult—if not impossible—in humans, animals are used alternatively. Although some animal pharmacokinetic studies with paclitaxel have been described, interpretation of the reported data is difficult. In most studies the radioactivity was quantified in the various biological samples after the administration of radiolabeled drug.^{12–14} Such methods, however, may be severely biased because they monitor the destiny of the radiolabel, which is not necessarily identical to that of the investigated drug. Eiseman *et al.*¹⁵ have used an HPLC procedure to quantify paclitaxel in plasma and tissues of mice. Their results showed a wide distribution to most tissues but the brain and testis in mice receiving 22.5 mg/kg of paclitaxel. They did not find direct evidence for non-linear pharmacokinetic behavior as observed in the clinical studies, since plasma pharmacokinetic parameters were similar in female mice receiving 11.25 or 22.5 mg/kg. Indirect evidence was obtained from the failure to achieve the predicted steady-state plasma level after continuous infusion. The poor sensitivity of their assay, however, prevented studies at dose levels below 11.25 mg/kg. Previous studies in humans and animals^{7,16,17} have indicated that paclitaxel is metabolized substantially. By using sensitive analytical methods, several hydroxylated paclitaxel metabolites in human plasma have been detected.^{7,10}

We have recently developed and validated a sensitive analytical method for the determination of paclitaxel and the principal human metabolites in a diverse array of biological matrices, based on reversed-phase HPLC and a highly selective sample pre-treatment procedure.¹⁸ This report describes the results of a detailed study of the tissue distribution, metabolism and excretion of paclitaxel performed in mice, using this HPLC methodology.

Materials and methods

Drugs and chemicals

Paclitaxel (batch 80617492D), 2'-methylpaclitaxel and paclitaxel formulated as a stock solution of 6 mg/ml (Taxol[®]) in 50% Cremophor EL in dehydrated ethanol USP were supplied by the Bristol-Myers Squibb (Princeton, NJ). Purity of the drugs

used in the experiments was checked by the analytical HPLC system described below. Paclitaxel metabolites 3'-*p*-hydroxypaclitaxel (**I**), 6 α -hydroxypaclitaxel (**II**) and 6 α ,3'-*p*-dihydroxypaclitaxel (**III**) have been isolated and purified from feces specimens obtained from patients receiving a 3 or 24 h i.v. infusion of paclitaxel at a dose level of 135 or 175 mg/m².¹⁹ Lyophilized bovine albumin powder (BSA) originated from Organon Teknica (Boxtel, The Netherlands). All chemicals were of analytical grade (methanol and acetonitrile were HPLC grade solvents) and were obtained from Merck (Darmstadt, Germany). Drug-free human plasma originated from the Central Laboratory of the Blood Transfusion Service (Amsterdam, The Netherlands). Water was purified by the Milli-Q Plus system (Waters, Milford, MA).

Pharmacokinetic study

Female FVB mice, 10–14 weeks of age, body weight 23–29 g, were used throughout all experiments, and were given food and water *ad libitum*. The animals were housed according to institutional guidelines. Paclitaxel formulated in Cremophor EL and ethanol (1:1, v/v) was diluted with isotonic sodium chloride to a final concentration of 0.6 or 3 mg/ml. The maximum volume of the diluted drug solution injected was always less than 200 μ l. Paclitaxel was administered at dose levels of 2, 10 or 20 mg/kg body weight by a single i.v. bolus injection in the tail vein under light diethyl ether anesthesia.

Blood and tissue specimens were obtained from four animals per time point at 0.5, 1, 4, 8, 24 and 48 h after drug administration. Blood was obtained under diethyl ether anesthesia from the retro-orbital venous plexus. The specimen was collected in 1.5 ml polypropylene microtubes (Eppendorf, Hamburg, Germany) containing 7 USP units lithium heparin and the tubes were centrifuged immediately (2100 g) for 10 min at 0°C using a Beckman Model J-6B/P centrifuge (Palo Alto, CA). The plasma supernatant was separated and stored at –20°C until analysis within 2 weeks. Brain, dorsal fat, muscle (back), breast, organ fat, colon, cecum, small intestine, stomach, liver, gall bladder (bile), kidneys, lungs, spleen, heart, ovary, uterus, thymus and lymph nodes were dissected and blotted dry. The fat, muscular tissues and other adhering visceral debris were carefully removed from the organ outersurface with tweezers. Tissue samples of the gastrointestinal tract were cleared from their contents and minced into small pieces using surgical

scissors. Each tissue sample was kept on ice, accurately weighed in polystyrene tubes and homogenized at 4°C in 5 or 10 volumes of 40 g/l BSA in water using a Biospec Products tissue homogenizer (Bartlesville, OK). Aliquots of the homogenates were stored at -20°C.

Excretion of paclitaxel and metabolites was studied at dose levels of 2, 10 and 20 mg/kg, using six mice per dose level. The mice were housed in Ruco Type M/1 metabolic cages (Valkenswaard, The Netherlands), and feces and urine was collected at ambient temperature at 12, 24, 48, 72 and 96 h after drug administration. Feces samples were homogenized in BSA as described above. Urine was diluted immediately 5-fold with drug-free human plasma and was frozen at -20°C.

Drug analysis

Paclitaxel and the metabolites **I**, **II** and **III** in plasma, tissues, urine and feces were determined according to the HPLC method reported in detail previously.¹⁸ In summary, sample pre-treatment involved the extraction of the analytes from 100–200 µl of plasma, 200–1000 µl of tissue homogenate, 50–200 µl of feces suspension or 1000 µl plasma-diluted urine twice with 4.0 ml diethyl ether in glass screw-cap tubes containing 25 µl of 20 µg/ml of 2'-methylpaclitaxel in methanol as internal standard. The combined organic layers were evaporated *in vacuo*, using a Savant SpeedVac® Plus SC210A system (Farmingdale, NY) at 43°C and the residue was reconstituted in 250 µl of drug-free human plasma by sonication for 3 min. Further sample processing was performed automatically using the ASPEC® system (Gilson Medical, Middleton, WI). Cyano Bond Elut solid phase extraction (SPE) columns were pre-conditioned with methanol and 0.01 M ammonium acetate buffer pH 5.0. A volume of 300 µl of 0.2 M ammonium acetate buffer pH 5.0 was added to the sample and 500 µl was loaded onto the SPE column. The columns were rinsed with 2 ml of 0.01 M ammonium acetate buffer pH 5.0 and 1 ml of methanol–0.01 M ammonium acetate buffer pH 5.0 (2:8; v/v). Paclitaxel, the internal standard and metabolites were eluted with 500 µl of a mixture of acetonitrile–triethylamine (1000:1; v/v). The solvent was evaporated and the residue was reconstituted in 200 µl of acetonitrile–methanol–water (4:1:5; v/v/v). An aliquot of 50 µl was subjected to chromatography. The reversed-phase chromatographic system consisted of Spectroflow SF400 solvent delivery system (Kratos, Ramsey, NJ), a Model

MSI660 autosampler (Kontron, Basel, Switzerland), and a Model 345 solvent recycler (Alltech, Deerfield, IL). Paclitaxel and metabolites were separated at ambient temperature using a stainless-steel analytical column (150 × 4.6 mm) packed with 5 µm APEX-octyl material (Jones Chromatography, CO). The mobile phase comprised a mixture of acetonitrile–methanol–0.02 M ammonium acetate buffer pH 5.0 (4:1:5; v/v/v) and was delivered at a flow rate of 1 ml/min. Detection was performed at 227 nm with a Spectroflow SF757 UV/VIS detector (Kratos) or with a Model 996 Photo Diode Array (PDA) detector (Waters, Milford, MA). Peak integration was done on a Spectra Physics SP4600 DataJet integrator connected to a WINner/286 chromatography work station (San Jose, CA).

The concentrations of paclitaxel and its metabolites **I**, **II** and **III** were determined from linear calibration curves, constructed in blank human plasma. The ratio of the peak areas of each of the compounds and the internal standard was used for quantitative computations. Accuracy and within and between-day precision were always less than 15%. The lower limits of quantification of paclitaxel and the metabolites **I** and **II** were 25–100 ng/g (ng/ml) for the various biological matrices.¹⁶ The AUCs in plasma and tissues were calculated using the linear trapezoidal rule upto the last data point with a detectable level of paclitaxel.

Results

The tissue levels of paclitaxel have been determined at several time points after i.v. administration of 2, 10 and 20 mg/kg of paclitaxel to female FVB mice (Tables 1–3). In most tissues the peak levels of paclitaxel were achieved within 0.5–1 h after drug administration and the progressively declined to undetectable levels within 24–48 h. The highest peak levels of paclitaxel were observed in the liver, kidney, lung, spleen, heart, gall bladder (bile) and small intestine. Apart from the liver and tissues of the gastrointestinal tract, substantial levels were present only in the ovaries, uterus and thymus 24 h after administration of 10 and 20 mg/kg of paclitaxel. A slow release from the brain was observed, although the maximum concentration of paclitaxel achieved in this organ was the lowest of all tissues. At higher dose levels, the occurrence of the peak level of paclitaxel in the gall bladder (bile) tends to be delayed. As indicated by Table 4, a 5-fold increase in the dose level (from 2 to 10 mg/kg) resulted in a highly non-linear 42-fold increase in the plasma AUC, whereas the drug AUC values

observed in the tissues increased only about 5- to 10-fold. A further 2-fold increase in the dose level resulted in a 4-fold higher AUC in plasma and in a 2- to 3-fold higher AUC in most tissues.

Besides paclitaxel two other major peaks were detected in the cecum, small intestine, liver, gall-bladder (bile) and feces, which were not detectable in plasma and other tissues. Both the chromatographic retention times of these compounds and their UV spectra, as determined by on-line UV-PDA, corresponded with **I** and **II**. The maximum levels of these compounds were found in the tissues sampled at 4 h after drug administration (Tables 5 and 6).

At the 2 mg/kg dose level, the excretion of unchanged paclitaxel in the urine was low ($0.29 \pm 0.10\%$; mean \pm SEM; $n=6$). Only trace amounts of metabolites **I** and **II** were detected in urine. A substantial fraction of the administered dose (2 mg/kg) was recovered in the feces either as unchanged drug ($58.2 \pm 3.4\%$) or as metabolite **I** or **II** (28.7%). The rate of fecal excretion was independent of the dose, with most of the drug being recovered within 24 h. At the higher dose levels, fecal excretion of unchanged paclitaxel and metabolites **I** and **II** was significantly reduced (Table 7). The fate of the remaining fraction of the drug, which was not recovered, is unknown. The analytical procedure did not reveal any other putative metabolic products.

Discussion

A striking non-linear increase in the plasma AUC was observed with increasing dose, especially between the dose levels of 2 and 10 mg/kg. The plasma levels achieved with these dose levels are the most relevant for the human situation, where non-linear pharmacokinetic behavior has been reported also.⁷⁻¹¹ The increased AUC and maximum concentration indicated both a saturation of the drug elimination and distribution processes. A possible explanation of such a behavior could be concentration-dependent plasma protein binding. However, *in vitro* binding of paclitaxel to human plasma, albumin and α_1 -acid glycoprotein at clinically relevant concentrations (i.e. 80–5000 ng/ml) was found to be concentration independent.²⁰ Because under normal conditions the tissue distribution will be driven by the levels in the central (plasma) compartment, non-linear increases in the plasma levels of cytotoxic agents like paclitaxel could be a potential hazard, since it may unexpectedly lead to serious drug-related side effects. However, our data show that the non-linearly increased plasma concentrations does not lead to a proportional increase in the levels of paclitaxel in tissues, in line with the concept of saturable distribution.¹⁰

Where the plasma AUC increases 42-fold when the administered dose is increased from 2 to

Table 1. Tissue distribution^a of paclitaxel in female FVB mice after i.v. administration of 2 mg/kg of paclitaxel (mean \pm SEM; $n=4$)

Tissue	0.5 h	1 h	4 h	8 h	24 h	48 h
Brain	119 \pm 38	65 \pm 23	ND	ND	—	—
Dorsal fat	1710 \pm 8	822 \pm 8	260 \pm 80	ND	—	—
Muscle (back)	931 \pm 364	488 \pm 27	112 \pm 72	ND	—	—
Breast	1260 \pm 124	1410 \pm 210	304 \pm 57	ND	—	—
Organ fat	1110 \pm 104	1250 \pm 174	251 \pm 112	ND	—	—
Colon	1440 \pm 1040	1020 \pm 383	569 \pm 141	313 \pm 144	ND	—
Cecum	1300 \pm 51	1760 \pm 43	2280 \pm 469	2660 \pm 478	ND	—
Small intestine	2360 \pm 900	2300 \pm 503	1820 \pm 507	841 \pm 134	ND	—
Stomach	1580 \pm 163	2090 \pm 228	571 \pm 22	361 \pm 52	ND	—
Liver	7200 \pm 694	7530 \pm 1050	1640 \pm 55	810 \pm 126	134 \pm 1	ND
Gall bladder (bile)	43700 \pm 13700	31200 \pm 392	39100 \pm 953	36900 \pm 762	ND	—
Kidneys	5060 \pm 1220	3760 \pm 552	353 \pm 39	238 \pm 82	ND	—
Lungs	6330 \pm 1320	1510 \pm 156	410 \pm 14	220 \pm 13	ND	—
Spleen	3260 \pm 716	2200 \pm 267	306 \pm 46	254 \pm 67	ND	—
Heart	2330 \pm 641	1130 \pm 91	319 \pm 17	ND	—	—
Ovary	657 \pm 102	942 \pm 279	384 \pm 95	350 \pm 102	ND	—
Uterus	711 \pm 67	946 \pm 386	641 \pm 99	186 \pm 19	ND	—
Thymus	242 \pm 4	342 \pm 13	160 \pm 28	165 \pm 15	ND	—
Lymph nodes	1260 \pm 293	1040 \pm 160	310 \pm 4	327 \pm 75	ND	—
Plasma ^b	453 \pm 33	218 \pm 24	41.8 \pm 5.7	ND	ND	—

^a Concentration in ng/g.

^b Concentration in ng/ml.

ND, not detectable; —, not done.

Table 2 Tissue distribution^a of paclitaxel in female FVB mice after i.v. administration of 10 mg/kg of paclitaxel (mean \pm SEM; $n = 4$)

Tissue	0.5 h	1 h	4 h	8 h	24 h	48 h
Brain	347 \pm 64	184 \pm 15	79 \pm 8	58 \pm 16	ND	—
Dorsal fat	14400 \pm 748	10300 \pm 1120	2140 \pm 408	730 \pm 100	ND	—
Muscle (back)	59900 \pm 724	4280 \pm 244	1120 \pm 66	510 \pm 72	ND	—
Breast	6690 \pm 115	7030 \pm 157	1600 \pm 105	759 \pm 129	ND	—
Organ fat	4260 \pm 406	5410 \pm 469	2000 \pm 323	1030 \pm 206	ND	—
Colon	7840 \pm 1420	6560 \pm 2170	3040 \pm 739	2060 \pm 186	375 \pm 56	ND
Cecum	5130 \pm 325	5480 \pm 361	7960 \pm 134	4180 \pm 1560	210 \pm 29	ND
Small intestine	11400 \pm 320	11600 \pm 735	5180 \pm 1120	3050 \pm 196	184 \pm 52	ND
Stomach	8900 \pm 410	7790 \pm 234	3420 \pm 258	1370 \pm 260	299 \pm 11	ND
Liver	45000 \pm 3600	46000 \pm 2060	5910 \pm 20	4000 \pm 265	901 \pm 17	ND
Gall bladder (bile)	132000 \pm 29100	97400 \pm 26800	245000 \pm 3320	129000 \pm 1280	ND	—
Kidneys	16900 \pm 487	14600 \pm 605	2670 \pm 469	1060 \pm 323	ND	—
Lungs	12300 \pm 742	9730 \pm 179	2200 \pm 631	801 \pm 14	ND	—
Spleen	10800 \pm 489	8440 \pm 294	2220 \pm 216	855 \pm 349	ND	—
Heart	10900 \pm 541	7580 \pm 403	1300 \pm 96	317 \pm 65	ND	—
Ovary	3210 \pm 471	3790 \pm 223	1970 \pm 105	1410 \pm 255	496 \pm 10	ND
Uterus	3880 \pm 565	5740 \pm 737	2970 \pm 251	2280 \pm 95	233 \pm 55	ND
Thymus	3900 \pm 198	3550 \pm 204	2460 \pm 143	1700 \pm 170	1087 \pm 106	ND
Lymph nodes	6580 \pm 355	4530 \pm 527	1820 \pm 61	1430 \pm 375	ND	ND
Plasma ^b	16750 \pm 1280	9717 \pm 726	812 \pm 168	81.9 \pm 8.1	ND	—

^a Concentration in ng/g.^b Concentration in ng/ml.

ND, not detectable; —, not done.

Table 3 Tissue distribution^a of paclitaxel in female FVB mice after i.v. administration of 20 mg/kg of paclitaxel (mean \pm SEM; $n = 4$)

Tissue	0.5 h	1 h	4 h	8 h	24 h	48 h
Brain	1160 \pm 105	589 \pm 81	242 \pm 19	189 \pm 36	79 \pm 1	ND
Dorsal fat	30500 \pm 5280	24300 \pm 2650	5330 \pm 949	1940 \pm 252	59 \pm 12	ND
Muscle (back)	14200 \pm 648	10200 \pm 1680	3590 \pm 236	1240 \pm 142	ND	—
Breast	19600 \pm 1720	14620 \pm 508	4300 \pm 1630	1610 \pm 35	ND	—
Organ fat	7250 \pm 1430	10700 \pm 1130	6890 \pm 1380	3080 \pm 826	ND	—
Colon	22700 \pm 2060	18700 \pm 3500	18300 \pm 1250	4840 \pm 433	913 \pm 138	ND
Cecum	18900 \pm 1350	11000 \pm 908	14900 \pm 882	10500 \pm 1020	864 \pm 339	ND
Small intestine	35900 \pm 2410	26700 \pm 4600	15300 \pm 371	10400 \pm 696	494 \pm 206	ND
Stomach	22900 \pm 2300	12700 \pm 282	10600 \pm 200	4410 \pm 1170	1250 \pm 572	ND
Liver	109000 \pm 6170	80400 \pm 7000	15800 \pm 3080	9400 \pm 735	2140 \pm 2	ND
Gall bladder (bile)	111000 \pm 14900	105100 \pm 32000	165000 \pm 23800	343000 \pm 11900	ND	—
Kidneys	40600 \pm 3370	29100 \pm 1790	9030 \pm 1290	3010 \pm 54	309 \pm 230	ND
Lungs	33800 \pm 2380	17200 \pm 907	9900 \pm 575	1750 \pm 777	238 \pm 31	ND
Spleen	30900 \pm 2750	13600 \pm 727	9380 \pm 310	2310 \pm 925	ND	—
Heart	29000 \pm 3480	13900 \pm 596	3550 \pm 139	892 \pm 143	ND	—
Ovary	13900 \pm 927	8840 \pm 804	6050 \pm 65	2920 \pm 34	1240 \pm 219	ND
Uterus	14500 \pm 1900	9440 \pm 1900	7200 \pm 384	4220 \pm 296	903 \pm 165	ND
Thymus	9720 \pm 374	6790 \pm 663	7210 \pm 1040	7040 \pm 914	3860 \pm 394	ND
Lymph nodes	18500 \pm 1040	10240 \pm 545	6800 \pm 358	4680 \pm 284	366 \pm 9	ND
Plasma ^b	48470 \pm 1870	30480 \pm 5830	8760 \pm 1370	435 \pm 59	ND	ND

^a Concentration in ng/g.^b Concentration in ng/ml.

ND, not detectable; —, not done.

Table 4 Calculated AUC (h mg/l) of paclitaxel in tissues after the i.v. administration of 2, 10 or 20 mg/kg of paclitaxel, the ratios AUC(10 mg/kg) and AUC(20 mg/g):AUC(2 mg/kg) are given within the parentheses (in case of linear pharmacokinetic behavior, these ratios should be 5 and 10, respectively)

Tissue	2 mg/kg	10 mg/kg	20 mg/kg
Brain	0.08	0.89 (11.1)	2.84 (35.5)
Dorsal fat	4.41	34.5 (7.8)	96.3 (21.8)
Muscle (back)	1.49	15.4 (10.3)	40.1 (26.9)
Breast	3.55	22.8 (6.4)	53.7 (15.1)
Colon	5.12	49.6 (9.7)	164 (32.0)
Cecum	17.1	89.5 (5.2)	193 (11.3)
Small intestine	13.2	76.1 (5.7)	226 (17.1)
Stomach	7.17	46.1 (6.4)	125 (17.4)
Liver	31.7	17.1 (5.4)	362 (11.4)
Kidneys	10.8	45.5 (4.2)	135 (12.5)
Lungs	7.68	32.5 (4.2)	101 (13.2)
Spleen	7.06	29.7 (4.2)	76.7 (10.9)
Heart	3.62	23.9 (6.6)	53.1 (14.7)
Ovary	4.02	33.2 (8.3)	82.7 (20.6)
Uterus	4.63	47.1 (10.2)	98.5 (21.3)
Thymus	3.54	42.5 (12.0)	143 (40.4)
Lymph nodes	4.21	20.5 (4.8)	101 (24.0)
Plasma	0.67	28.4 (42.3)	109 (162.7)

10 mg/kg, most tissues show only a moderate 5- to 10-fold higher AUC. Although such non-linear increases in AUC might be caused by a saturation of enzymes involved in drug elimination, we think that it is caused by the substantial amounts of the vehicle Cremophor EL, co-administered with paclitaxel. Such an effect of Cremophor EL on drug elimination does not appear to be unique for paclitaxel, since it has also been reported for doxorubicin²¹

and for the photosensitizer C8KC.²² Several possible mechanisms may attribute to the alterations induced by Cremophor EL. A possibility, which would explain both manifestations of saturable elimination and the apparent saturable distribution, would be that higher levels of Cremophor EL reduce the 'free' fraction of the drug in plasma. It is known that Cremophor EL is capable of forming micelles in aqueous solutions, which may even persist for many hours after dilution below the critical micellar concentration.²³ These micelles can act as drug carriers which slowly release encapsulated paclitaxel from their contents. Alternatively, recent studies reported that Cremophor EL can cause a dissociation of serum lipoproteins and form products, which possess a very high affinity for compounds like C8KC and paclitaxel.^{22,24} Cremophor EL is capable of reversing P-glycoprotein mediated multi-drug resistance.²⁵⁻²⁸ Modulation of P-glycoprotein in the liver and/or the gastrointestinal tract may explain the reduced clearance at higher dose levels. It would, however, not explain the apparently saturable distribution. The role of the vehicle on the pharmacokinetics of paclitaxel is currently under further investigation.

Based on *in vitro* data from rat and human microsomal metabolism studies of paclitaxel, a substantial metabolism of paclitaxel to hydroxylated compounds would be expected.²⁹⁻³² However, a study by Eiseman *et al.*¹⁵ using HPLC with UV detection in CD2F1 mice given 22.5 mg/kg of paclitaxel did not report the presence of any metabolites. This was likely due to the poor sensitivity of the analytical

Table 5 Tissue distribution^a of metabolite I in female FVB mice after i.v. administration of 2, 10 or 20 mg/kg of paclitaxel (mean \pm SEM; n=4)

Tissue	0.5 h	1 h	4 h	8 h	24 h
Dose: 2 mg/kg					
cecum	ND	ND	ND	ND	ND
small intestine	ND	ND	ND	ND	ND
liver	372 \pm 89	877 \pm 35	695 \pm 10	ND	ND
gall bladder	12200 \pm 2560	11300 \pm 1090	9990 \pm 201	10800 \pm 185	ND
Dose: 10 mg/kg					
cecum	ND	ND	1900 \pm 301	1000 \pm 56	ND
small intestine	129 \pm 6	437 \pm 2	576 \pm 71	189 \pm 15	ND
liver	408 \pm 27	1430 \pm 243	1940 \pm 20	ND	ND
gall bladder	8570 \pm 845	7480 \pm 853	46700 \pm 5320	27800 \pm 1190	ND
Dose: 20 mg/kg					
cecum	ND	ND	4020 \pm 38	1720 \pm 162	ND
small intestine	211 \pm 8	815 \pm 15	1250 \pm 276	401 \pm 98	ND
liver	717 \pm 73	2810 \pm 535	2980 \pm 136	689 \pm 173	ND
gall bladder	6190 \pm 354	21900 \pm 1410	63400 \pm 12600	108000 \pm 28600	ND

^a Concentration in ng/g.

ND, not detectable.

Table 6 Tissue distribution^a of metabolite II in female FVB mice after i.v. administration of 2, 10 or 20 mg/kg of paclitaxel (mean \pm SEM; n = 4)

Tissue	0.5 h	1 h	4 h	8 h	24 h
Dose: 2 mg/kg					
cecum	ND	ND	ND	ND	ND
small intestine	ND	ND	ND	ND	ND
liver	104 \pm 3	511 \pm 27	258 \pm 32	ND	ND
gall bladder	5180 \pm 126	6330 \pm 1180	4910 \pm 476	6620 \pm 107	ND
Dose: 10 mg/kg					
cecum	ND	ND	830 \pm 113	841 \pm 139	ND
small intestine	53 \pm 1	184 \pm 9	355 \pm 64	104 \pm 4	ND
liver	244 \pm 12	826 \pm 140	1640 \pm 6	ND	ND
gall bladder	6870 \pm 1220	4730 \pm 340	31200 \pm 348	40300 \pm 2380	ND
Dose: 20 mg/kg					
cecum	ND	ND	1700 \pm 119	1520 \pm 68	ND
small intestine	93 \pm 3	308 \pm 66	801 \pm 82	220 \pm 4	ND
liver	453 \pm 70	1320 \pm 408	2270 \pm 249	404 \pm 110	ND
gall bladder	3080 \pm 163	10800 \pm 353	42900 \pm 3110	79800 \pm 22800	ND

^a Concentration in ng/g.
ND not detectable.

Table 7 Cumulative excretion (0–96 h) of paclitaxel and metabolites I and II into urine and feces after i.v. administration of 2, 10 and 20 mg/kg of paclitaxel (n = 6)

Route of excretion	Percentage of dose excreted at		
	2 mg/kg (mean \pm sem)	10 mg/kg (mean \pm sem)	20 mg/kg (mean \pm sem)
Urine			
Paclitaxel	0.29 \pm 0.10	0.26 \pm 0.03	0.23 \pm 0.03
metabolite I	ND	trace	trace
metabolite II	ND	trace	trace
Feces			
paclitaxel	58.2 \pm 3.4	51.4 \pm 5.7	44.5 \pm 1.1
metabolite I	17.7 \pm 1.8	15.4 \pm 1.3	8.2 \pm 0.3
metabolite II	11.1 \pm 1.5	10.1 \pm 1.3	8.2 \pm 0.3

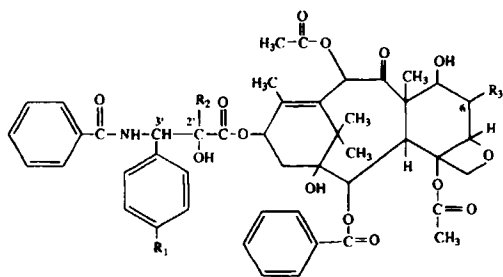
ND, not detectable.

procedure employed, as we detected two paclitaxel metabolites, i.e. I and II in cecum, small intestine, liver, gall bladder (bile) and feces. Although III, isolated from human feces, was not detected, the spectrum of metabolites formed in mice resembles that of humans more closely than in rats, in which 2-*m*-hydroxypaclitaxel is the major metabolite.^{16,17,29,33,34} Therefore, despite the fact that, in humans metabolite II is the principal metabolite, the mouse appears to be a more suitable model for metabolism studies than the rat.

The finding that metabolites I and II were not detectable in the plasma or any of the other tissues indicate that the major part of these metabolites is excreted directly into the bile and that reabsorption from the intestinal lumen is minimal. The amounts

of metabolites I and II excreted in the feces accounted for about 25% of the administered dose. Together with their reduced cytotoxic activity in *in vitro* clonogenic assays as shown previously,^{19,33} these results indicate that 3'-*p*- and 6 α -hydroxylation of paclitaxel are important detoxification pathways.

At 0.5 h after drug administration, the highest levels of paclitaxel were found in the liver, gall bladder and small intestine, which is consistent with an effective hepatobiliary extraction.¹² Consequently, the major part of the administered drug is recovered in the feces. Although high levels of paclitaxel are attained in the kidney, this does not result in a substantial renal excretion of the parent compound. The fecal excretion and biliary excretion rate were markedly reduced at the higher dose levels. Recent



compound	R ₁	R ₂	R ₃
paclitaxel	H	H	H
3'-p-hydroxypaclitaxel	OH	H	H
6α-hydroxypaclitaxel	H	H	OH
6α,3'-p-dihydroxypaclitaxel	OH	H	OH
2'-methylpaclitaxel	H	CH ₃	H

Figure 1. Chemical structures of paclitaxel, its metabolites 3'-p-hydroxypaclitaxel, 6α-hydroxypaclitaxel, and 6α,3'-p-dihydroxypaclitaxel, the internal standard 2'-methylpaclitaxel.

studies in anesthetized male Wistar rats showed that Cremophor EL caused cholestasis related to a reduction in both bile acid-dependent and bile-acid-independent bile flow, probably due to transitory hepatotoxic effects.³⁵ Alternatively, the dose-dependent fecal excretion of paclitaxel and metabolites **I** and **II** might be related to a saturation of transport proteins involved in the biliary excretion. The metabolic fate of the fraction of drug that is not recovered as parent compound or as metabolite **I** or **II** is currently under investigation.

Acknowledgment

The authors are indebted to Mr AJ Schrauwers for excellent bio-technical assistance.

References

- McGuire WP, Rowinsky EK, Rosenheim NB, *et al.* Taxol: a unique antineoplastic agent with significant activity in advanced ovarian epithelial neoplasms. *Ann Intern Med* 1989; **111**: 273–81.
- Holmes FA, Walters RS, Theriault RL, *et al.* Phase II trial of taxol, an active drug in the treatment of metastatic breast cancer. *J Natl Cancer Inst* 1991; **83**: 1797–804.
- Chang A, Kim K, Glick J, *et al.* Phase II study of taxol, merbarone, and piroxantrone in stage IV non-small cell lung cancer: the Eastern Cooperative Oncology Group (ECOG) results. *J Natl Cancer Inst* 1993; **85**: 388–93.
- Rowinsky EK, Burke PJ, Karp JE, *et al.* Phase I and pharmacodynamic study of taxol in refractory acute leukemias. *Cancer Res* 1989; **49**: 4640–7.
- Rose WC. Taxol: a review of its preclinical antitumor activity. *Anti-Cancer Drugs* 1992; **3**: 311–21.
- Spencer CM, Faulds C. Paclitaxel. A review of its pharmacodynamic and pharmacokinetic properties and therapeutic potential in the treatment of cancer. *Drugs* 1994; **48**: 794–847.
- Huizing MT, Keung ACF, Rosing H, *et al.* Pharmacokinetics of paclitaxel and metabolites in a randomized comparative study in platinum-pretreated ovarian cancer patients. *J Clin Oncol* 1993; **11**: 2127–35.
- Jamis-Dow CA, Klecker RW, Sarosy G, *et al.* Steady-state plasma concentrations and effects of taxol for a 250 mg/m² dose in combination with granulocyte-colony stimulating factor in patients with ovarian cancer. *Cancer Chemother Pharmacol* 1993; **33**: 48–52.
- Sonnichsen DS, Hurwitz CA, Pratt CB, *et al.* Saturable pharmacokinetics and paclitaxel pharmacodynamics in children with solid tumors. *J Clin Oncol* 1993; **12**: 532–8.
- Gianni L, Kearns CM, Capri G, *et al.* Nonlinear pharmacokinetics and metabolism of paclitaxel and its pharmacokinetic/pharmacodynamic relationships in humans. *J Clin Oncol* 1995; **13**: 180–90.
- Ohtus T, Sasaki Y, Tamura T, *et al.* Clinical pharmacokinetics and pharmacodynamics of paclitaxel: a 3-hour infusion versus a 24 hour infusion. *Clin Cancer Res* 1995; **1**: 599–606.
- Klecker RW, Jamis-Dow CA, Egorin MJ, *et al.* Effect of cimetidine, probenecid, and ketoconazole on the distribution, biliary secretion, and metabolism of [³H]Taxol in the Sprague-Dawley rat. *Drug Metab Dispos* 1994; **22**: 254–8.
- Lesser GJ, Grossman SA, Eller S, *et al.* Distribution of ³H-Taxol in the nervous system and organs of rats. *Proc Am Soc Clin Oncol* 1993; **12**: 160.
- Gaver RC, Deeb G, Willey T, *et al.* The disposition of paclitaxel (taxol) in the rat. *Proc Am Ass Cancer Res* 1993; **34**: 390.
- Eiseman JL, Eddington ND, Leslie L, *et al.* Plasma pharmacokinetics and tissue distribution of paclitaxel in CD2F1 mice. *Cancer Chemother Pharmacol* 1994; **34**: 465–71.
- Monsarrat B, Alvinerie P, Wright M, *et al.* Hepatic metabolism and biliary clearance of taxol in rats and humans. *J Natl Cancer Inst Monogr* 1993; **15**: 39–46.
- Monsarrat B, Mariel E, Cros S, *et al.* Isolation and identification of three major metabolites of taxol in rat bile. *Drug Metab Dispos* 1990; **18**: 895–901.
- Sparreboom A, Van Tellingen O, Nooijen WJ, *et al.* Determination of paclitaxel and metabolites in mouse plasma, tissues, urine and faeces by semi-automated reversed-phase high-performance liquid chromatography. *J Chromatogr* 1995; **664**: 383–91.
- Sparreboom A, Huizing MT, Boessen JJB, *et al.* Isolation, purification, and biological activity of mono- and dihydroxylated paclitaxel metabolites from human faeces. *Cancer Chemother Pharmacol* 1995; **36**: 299–304.
- Kumar G, Walle UK, Bhalla KN, *et al.* Binding of taxol to human plasma, albumin and α₁-acid glycoprotein. *Res Commun Chem Pathol Pharmacol* 1993; **80**: 337–44.
- Webster LK, Millward MJ, Cosson EJ, *et al.* Cremophor EL changes the pharmacokinetics of doxorubicin. *Proc Am Ass Cancer Res* 1995; **36**: 290.

22. Woodburn K, Chang CK, Lu S, *et al.* Biodistribution and PDT efficacy of a ketochlorin photosensitizer as a function of the delivery vehicle. *Photochem Photobiol* 1994; **60**: 154–9.
23. Kessel D. Properties of Cremophor EL micelles probed by fluorescence. *Photochem Photobiol* 1992; **56**: 447–51.
24. Sykes E, Woodburn K, Decker D, *et al.* Effects of Cremophor EL on the distribution of taxol to serum lipoproteins. *Br J Cancer* 1994; **70**: 401–4.
25. Woodcock DM, Jefferson S, Linsenmeyer ME, *et al.* Reversal of the multidrug resistance phenotype with Cremophor EL, a common vehicle for water-insoluble vitamins and drugs. *Cancer Res* 1990; **50**: 4199–203.
26. Schuurhuis GJ, Broxterman HJ, Pinedo HM, *et al.* The polyoxyethylene castor oil Cremophor EL modifies multidrug resistance. *Br J Cancer* 1991; **62**: 591–4.
27. Friche E, Jensen PB, Sehested M, *et al.* The solvents Cremophor EL and Tween 80 modulate daunorubicin resistance in the multidrug resistant kEhrlich ascites tumor. *Cancer Commun* 1990; **90**: 297–303.
28. Ross DD, Wooten PJ, Tong Y, *et al.* Synergistic reversal of multidrug-resistance phenotype in acute myeloid leukemia cells by cyclosporin A and Cremophor EL. *Blood* 1994; **83**: 1337–47.
29. Walle T, Kumar GN, McMillan JM, *et al.* Taxol metabolism in rat hepatocytes. *Biochem Pharmacol* 1993; **49**: 1661–64.
30. Cresteil T, Monsarrat B, Alvinerie P, *et al.* Taxol metabolism by human liver microsomes: identification of cytochrome P450 isozymes involved in its biotransformation. *Cancer Res* 1994; **54**: 386–92.
31. Harris JW, Rahman A, Kim B-R, *et al.* Metabolism of taxol by human hepatic microsomes and liver slices: participation of cytochrome P450 3A4 and an unknown P450 enzyme. *Cancer Res* 1994; **54**: 4026–35.
32. Rahman A, Koczekwa KR, Grogan J, *et al.* Selective biotransformation of taxol to 6 α -hydroxytaxol by human cytochrome P450 2C8. *Cancer Res* 1994; **54**: 5543–6.
33. Harris JW, Katki A, Anderson LW, *et al.* Isolation, structural determination, and biological activity of 6 α -hydroxytaxol, the principal human metabolite of taxol. *J Med Chem* 1994; **37**: 706–10.
34. Kumar GN, Oatis JE, Thornburg KR, *et al.* 6 α -Hydroxytaxol: isolation and identification of the major metabolite of taxol in human liver microsomes. *Drug Metab Dispos* 1994; **22**: 177–9.
35. Roman ID, Monte MJ, Esteller A, *et al.* Cholestasis in the rat by means of intravenous administration of cyclosporine vehicle, Cremophor EL. *Transplantation* 1989; **48**: 554–8.

(Received 7 September 1995; accepted 25 September 1995)